International Journal of Innovative
Computing, Information and Control
Volume 8, Number 1(B), January 2012

 ISSN 1349-4198
pp. 867–893

ELECTRONIC DESIGN OF PORTABLE ECT FOR CRUDE PALM OIL QUALITY MONITORING SYSTEM

ELMY JOHANA[1], RUZAIRI ABDUL RAHIM[2], MOHD. HAFIZ FAZALUL RAHIMAN[3] AND SITI ZARINA MOHD. MUJI[1]

[1]Department of Robotic and Mechatronic Engineering
Faculty of Electrical Electronics Engineering
Universiti Tun Hussein Onn Malaysia
Parit Raja, Batu Pahat, Johor 86400, Malaysia
{elmy; szarina}@uthm.edu.my

[2]Process Tomography and Instrumentation Research Group, Cybernetics Research Alliance
Faculty of Electrical Engineering
University of Technology Malaysia
UTM Skudai, Johor 81310, Malaysia
ruzairi@fke.utm.my

[3]School of Mechatronic Engineering
Universtiti Malaysia Perlis
Kampus Ulu Pauh, Arau, Perlis 02600, Malaysia
hafiz@unimap.edu.my

Received October 2010; revised February 2011

ABSTRACT. *This paper presents the process of visualizing the composition of a crude palm oil (CPO) during separator process which collects the recovered crude palm oil from the liquid waste before separation process, in order to monitor the percentage of load waste present using a tomographic technique by Portable Electrical Capacitance Tomography (ECT) so that the process separation (separate oil and water/sludge) becomes much easier and the quality of crude palm oil can be reliably monitored. Palm oils industry is one of the largest production, producer and exporter of palm oil and palm oil products countries in the world. Oil Palm was first introduced to Malaysia in year 1875 as an ornamental plant. Malaysia has the most ideal climate conditions for growing oil palm. The growth of the palm oil industry in Malaysia has been phenomenal over the last 4 decades. Nevertheless, palm oil industry is one of the most pollution generating agro industries in Malaysia. One of the major problems arises from the oil palm fruit processing is the large amount of wastes generated during the processes. There are two main wastes resulted from operation of a Palm Oil Mill, namely solid waste and liquid waste. The solid waste may consist of palm Kernel shells, mesocarp fibers and empty fruit bunches. The liquid waste generated from extraction of palm oil of a wet process comes mainly from oil room after separator or decanter. There is no monitoring system that is currently available in our local palm oil mill to visualize the percentage of load waste present inside the vessel. Therefore, the system is aimed to become an instrument to support the local and foreign palm oil mills to efficiently control in monitoring the quality of crude palm oil flow in the conveying pipeline during extraction of palm oil mill process. The monitoring system is able to visualize the percentage of load waste present inside the vessel so that the data can be used to design better process equipment in mill process or to control certain processes in order to maximize the quality of crude palm oil and the POME treatment process can be improved.*

Keywords: Portable ECT, Crude palm oil, POME, Monitoring system

1. **Introduction.** The Electrical Capacitance Tomography, ECT technique has been widely studied since the early 90's. Research work has proved that this technique is one of the most attractive and promising methods for the measurement of two-phase flow, because of its non-invasion, reliability, simplicity and high-speed capabilities [1]. It has been used to achieve real-time visualization of industrial processes and void fraction measurement of two-phase flow. ECT can be used for imaging industrial multi-component processes involving non-conducting fluids and solids in pipelines [2]. Generally, ECT is a technique to obtain information about the distribution of the contents within closed pipes or vessels by measuring the variations in the dielectric properties of the material inside the vessel [3]. The main principle in ECT is based on determining the variations in capacitance within the measurement section, which is a function of the permittivity of the medium between the electrode plates over the entire sensing volume. The spatial resolution of a tomographic imaging system depends on the number of independent measurements and fineness of sensitivity focus for each measurement. The measured values or data are manipulated to reconstruct the cross sectional image of the pipeline using a computer program [4].

ECT has been used in many applications especially in chemical and petroleum industry, including multiphase flow in the oil pipeline. Looking forward to other applications instead of gas, petroleum and pharmaceutical industries, palm oil mill production also can be seen as a potential approach to be implemented. The palm oil industries processing has not been monitored previously with ECT. This is probably not every country involves with palm oil production. In this research, the monitoring of the concentration of recovery palm oil was utilized with ECT. Malaysia is the biggest palm oil production, producer and exporter of palm oil and palm oil products country in the world (Malaysia Palm Oil Board, 2003). Malaysia has produced almost 17.0 million tons of crude palm oil in 2010 from oil palm planted area of 4.69 mil hectares and almost 420 of palm oil mills. The palm oil industry generated revenue of app. RM 65 billion (2010) which was the largest agricultural sectors contributor for Malaysia. The palm oil milling industry for the CPO production has adopted mechanical means of extraction technology. The technology of palm oil milling has not seen much changes since the first establishment of palm oil mills in early 1950's, as first reported in Mongana and Stork reports (Sime Darby Research Sdn. Bhd., 2011).

Crude Palm oil is produced from palm fresh fruit bunches (PFFB) through major operational processes such as steaming and squeezing. During the processing of the fresh fruit bunches (FFB), water is the most needed resource. It has been reported that processing/milling of one ton of FFB requires 1.5 m^3 of water, and 50% of the water used during milling is released as liquid waste while the rest is lost as steam in the boilers blow down, wash waters and leakage (Industrial Processes and the Environmental Handbook No. 3, 1999) [5]. The liquid waste combined with the wastes from sterilizer condensate and cooling water is called palm oil mill effluent (POME). POME is high volume liquid waste which is non-toxic, organic in nature but has an unpleasant odor and is high polluting [6]. Generally, operation of the palm oil mill generates many by-products and liquid waste which may pose a significant impact on the environment if they are not dealt with properly. In Malaysia, for example, 9.9 million tons of solid waste consisting of empty fruit bunch (EFB), fiber and fruit shell and approximately 20 million tons of palm oil mill effluent (POME) are generated every year. The palm oil industry is the worst source of water pollution.

The POME has acidic (pH 4-5), has discharge temperature of 80-90°C/50-60°C and is non toxic (since no chemicals are added during extraction) [5]. Currently, the majority of palm oil mills have adopted conventional biological treatment of anaerobic or facultative

digestion which needs a large treatment area and a long treatment period about 80 to 20 days [6]. The treatment called as biological ponding system or the lagoon system is developed rapidly as a typical POME treatment system in Malaysia. This system consists of dealing with ponds, anaerobic, facultative and aerobic ponds. The ponding system normally requires long retention time in excess of 20 days, the biogas is released into the atmosphere, and an average of 36% methane gas is emitted into the atmosphere from the open tank digester. The methane gas produced by the open tank digester and lagoon system is 35% and 45% respectively. The methane emission from the palm oil industry is the largest green house gas (GHG) source in Malaysia. Carbon emission credit can be earned for reducing GHG emission [7]. Figure 1 shows the biological ponding system in palm oil milling.

FIGURE 1. Biological ponding system palm oil milling, sime darby research Sdn. Bhd. Carey Island, Banting Selangor, Malaysia, 2011

The above pollution can be minimized by reducing the amount of palm oil mill effluent (POME). However, the POME or waste matter such as water, volatile matter, dirt or sludge cannot be reliably monitored inside the vessel before separation process in our palm oil mill today, and there is no monitoring system that is currently available in our local palm oil mill to visualize the percentage of liquid waste present inside the vessel. Figure 2(a) shows the flow diagram of palm oil milling process at Sime Darby Research Sdn. Bhd. Carey Island and Figure 2(b) shows the crude palm oil (CPO) process.

The liquid waste generated from extraction of palm oil of a wet process comes mainly from oil room. After extraction process, the CPO needs to be clarified before it goes to refining process. The clarifying process is to separate the crude palm oil from sludge or load waste using gravity technology as shown in Figure 3. The light oil will stay at the top of the tank and the heavy oil (mix with liquid waste/sludge) will remain at the bottom as shown in Figure 3.

The oil at the top will go to the purifier to have clean CPO and the remaining oil which mixes with the sludge/liquid waste will be sent to recovery process through Decanter which is to recover remaining oil from the sludge/liquid waste. The Decanter is used to collect oil from the liquid waste before it goes to separation process (separate between oil and sludge/liquid waste). The purpose of the system is to monitor the percentage of load waste present after Decanter so that the process separation (separate oil and water/sludge) will be more effective and the quality of crude palm oil can be reliably

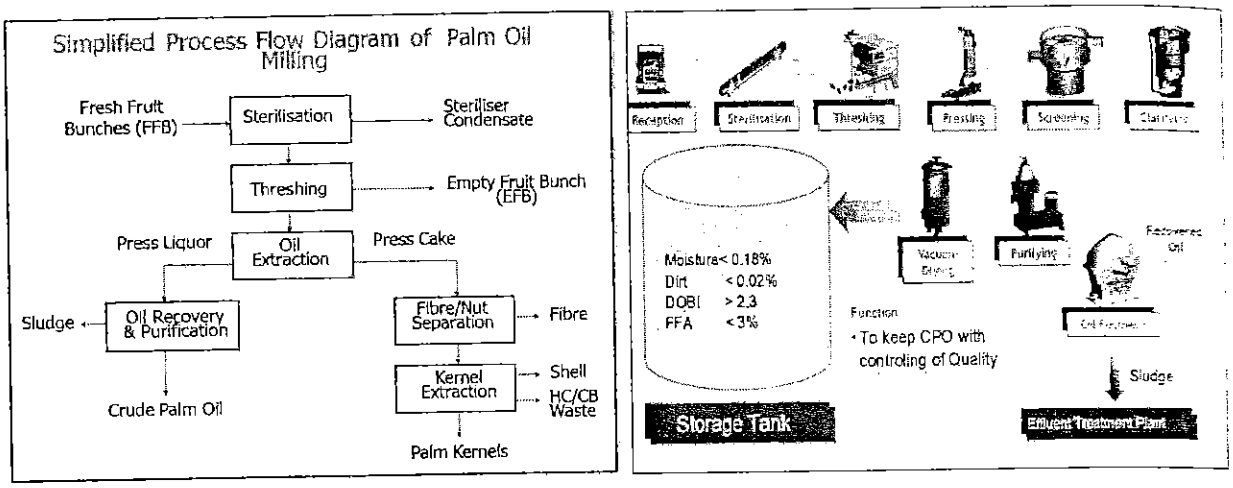

FIGURE 2. (a) Flow diagram of palm oil milling and (b) crude palm oil process-sime darby research Sdn. Bhd., Carey island, Banting Selangor, Malaysia, 2011

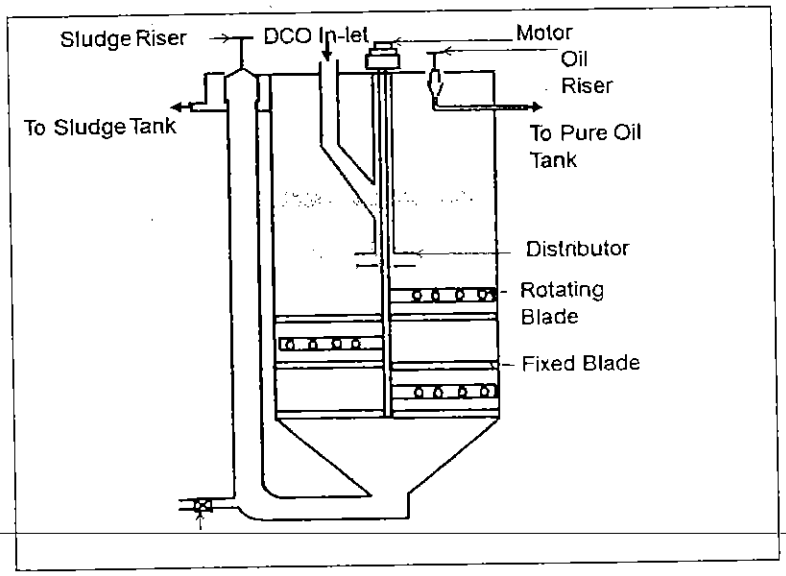

FIGURE 3. Clarifier tank

monitored. The visualization results provide information about the flow regime and concentration distribution. Such information can assist in the design of process equipment, verification of existing computational modeling and simulation techniques or to assist in process control and monitoring in order to improve the quality of crude palm oil and the POME treatment process being more efficient.

Therefore, this work aims to experimentally investigate the capability of using 16 electrodes of Portable Electrical Capacitance Tomography (ECT) to identify the flow pattern and to obtain the phase concentration of crude palm oil related multiphase systems (crude palm oil/water and crude palm oil/gas). The acquired concentration profile that obtains from capacitance measurements is able to image liquid and gas mixture in the pipeline. In the previous research of ECT, all the electrode sensors were built fixed on the vessel.

The electrode plate cannot be moved to other vessels, and the installation must be done on the actual vessel. The electrode plates which act as the sensor have been assembly fixed on the pipeline, thus it causes difficulty for the production to have any new process installation in the future. The new on-board sensing plate offers a new design and idea on ECT system which is portable to be assembled in different diameter sizes of pipeline, and it is flexible to apply in any number due to different sizes of pipeline without redesigning the sensing module then the sensor could be worked independently. This research has broken the limitation and started another new generation in the ECT world, portable ECT system that can be loaded on any vessel in a second which will enable on-line *in situ* ECT inspections with a low-cost portable system.

2. **Portable ECT Development.** This research is aimed at investigating the use of a portable sensor design for use in an ECT system. As shown in Figure 1, the project can be divided into 3 stages, which are the portable sensor design, the central control unit design and software programming.

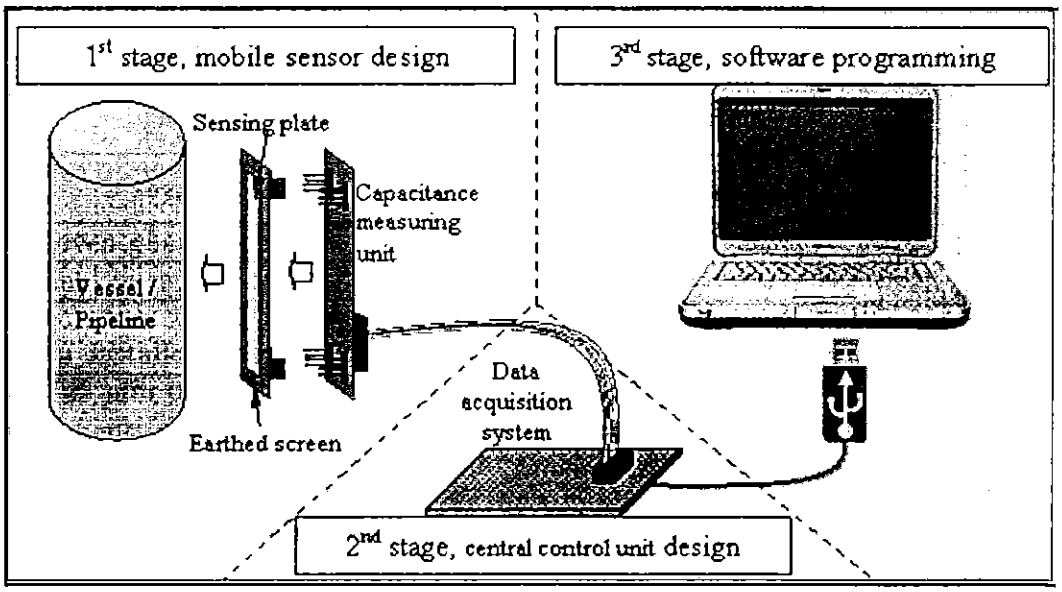

FIGURE 4. Overview of the project

A typical ECT system consists of a sensor built up from 8, 12 or 16 electrodes, capacitance measurement circuit, central control unit and a control PC [8]. The electrode which is normally built from conductive plate acts as sensing surface that direct contact to the measuring area. The electrode provides excitation signals and converts the capacitances into voltage signals, which are conditioned and then digitized for data acquisition. The capacitance measuring circuit or better known as signal conditioning circuit is used to collect data and convert the measurement readings to digital. A central control unit is designed to synchronize all the operations and transfer the data to a control PC. A control PC that receive the measurements reading will store the acquired data, reconstruct images from the integral measurements and take action feedback to control the flow [9].

ECT is appropriate for imaging industrial multi-component processes which involve non-conducting flow materials. The main principle in ECT is based on the standing capacitance, which is a function of the permittivity of the medium between the electrode plates over the entire sensing volume [9]. The spatial resolution of a tomographic imaging system depends on the number of independent measurements and fineness of sensitivity

focus for each measurement. The measured values or data will be manipulated to reconstruct the cross sectional image of the pipeline by computer programming [4]. This paper will focus on the sensing module development in order to visualize the cross sectional image of crude palm oil flow inside a closed pipe.

3. **Portable Sensor Design.** Typical ECT sensors must have a high level of mechanical stability, because any small movement between electrodes will change the values of inter-electrode capacitances. In the previous research in ECT, all the electrode sensors were built fixed on the vessel. The electrode plate cannot be moved to other vessel, and the installation must be done on the actual vessel. This research has broken the limitation, start another new generation in the ECT world, portable ECT system that can be load on any vessel in a second. Because of this feature, number of the electrode sensors can be selected depends on the diameter of the pipeline. The material of the electrode must be highly conductive material, such as copper, aluminum, silver, brass, tungsten and iron. Table 1 shows comparison between some high conductivity materials. Copper has been chosen because it can be found on any bare Printed Circuit Board (PCB). Despite the fact that the copper is a highly conductive material, which is desirable in an ECT system, the cost of this material is low and it is easy to be fabricated.

TABLE 1. Typical electrical conductivities

Conductor	Electrical Conductivity ($S.m^{-1}$)	Temperature (°C)
Silver	63.01×10^6	20
Copper	59.6×10^6	20
Annealed Copper	58.0×10^6	20
Aluminum	37.8×10^6	20
Brass	25.6×10^6	28

In an ideal ECT sensor, the electric field lines will be normal to the sensor axis. However, if the electrodes used are short compared to the diameter of the sensor, the electromagnetic field lines will spread out at the ends of the electrodes. This will have two consequences: First, the capacitance measured between electrodes will be reduced and hence the measurement sensitivity will also be reduced. Second, the axial resolution of the sensor will be degraded because of the axial spreading of the field lines at the end of the electrodes. The purpose of the guard electrodes is to maintain a parallel electric field pattern across the sensor in the region of the measuring electrodes, by preventing the electric field lines from spreading axially at the ends of the measuring electrodes. This improves both the axial resolution and the sensitivity of the sensor. Other than that, earthed guard electrode tracks may also be needed between adjacent measuring electrodes to reduce the standing capacitance between adjacent electrodes to a value low enough to avoid overloading or saturating the capacitance measuring system. These guard electrodes are connected to guard driving circuitry on the data acquisition module. Figure 5 shows the driven guard electrode design for an 8-electrode sensor.

In this research, 16 electrodes developed by using special design PCB, as shown in Figure 6. The sensor module is made by a double layer copper plated FR4 ($\varepsilon_r = 4.6$) PCB with the thickness of 1.6 mm. The FR4 is a widely used stiffener for flexible PCB and it is cost efficient solution for high-end application involving impedance control and high frequency. Compare with the past design on ECT system, the new electrode sensor

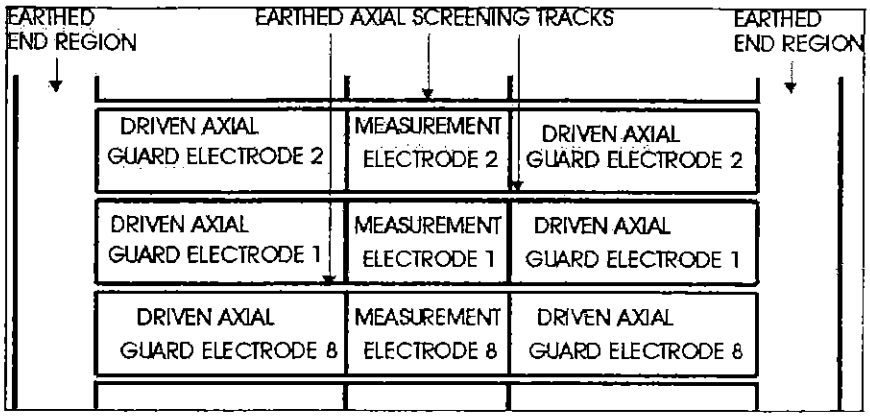

FIGURE 5. Driven guard electrode design for an 8-electrode sensor

no longer be bended and stick on the pipe wall. This sensor arranged symmetrically in hexadecagon surrounding the pipeline. Each electrode sensing has 19 mm in width, and 100 mm in length sensor area, copper and driven. The 100 mm length of sensor is chosen because the axial length of electrodes is related to inter-electrode capacitance, signal bandwidth and measurement uncertainty of measured media. Longer electrodes produce an average signal over a greater axial length, which results in bad dynamic performance. Shorter electrode may result in capacitance too small to be measured accurately [10] and normally, the electrode length is chose as 10 cm [11].

The driven guard has been intergraded onto electrode sensor in order to prevent the electric field lines from spreading at the ends of the measuring electrodes. These driven guard electrodes will surround the circumference of the pipeline once all the 16 electrodes have been installed on pipeline. The length of the guard electrodes is 33 mm on the left, and 43 mm on the right, as shown in Figure 6. The measuring electrodes must be completely surrounded by an earthed, metal screen so that the signals obtained in the signal conditioning circuit will not be influenced by the disturbance in the air. In this research, the earth screen is located on the top layer of the electrode PCB as shown in Figure 7. These sensing plates are covered by an insulated metal screen called the earth screen. The material used for the sensing and screen layers is a copper surface designed using double layer Printed Circuit Board (PCB). The earth screen covers the all the surface on the top layer. Based on the concept, the electrode sensor for ECT is created, by using special design PCB, as shown in Figure 7.

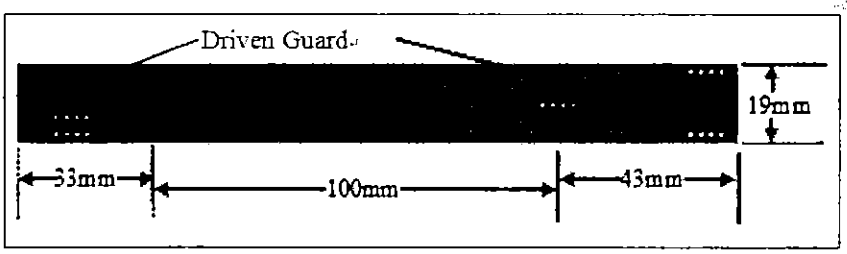

FIGURE 6. Electrode's dimension

4. **Electrodes Connecting Techniques.** Accurate data is only get with a good design in sensing electronics that able to eliminate noises. An important issue with instrumentation design is the performance of the circuit in the presence of noise, which is generated by external interference and thermal effects within components [3]. An ideal capacitance

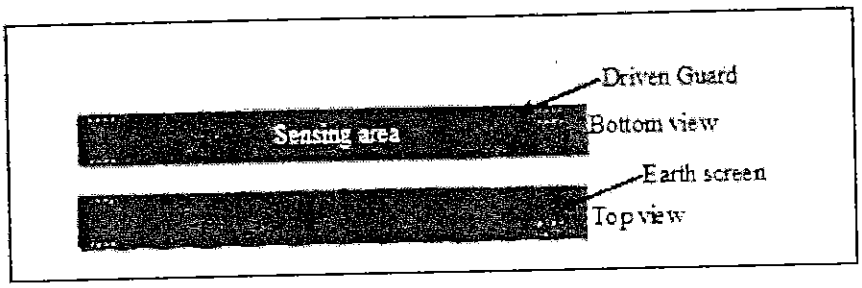

FIGURE 7. An overview of a complete electrode sensor design

measuring system will have a very low noise level, a wide dynamic measurement range and high immunity to stray capacitance. The capacitance value in measured would be from the range from a few to hundreds fem to farads.

In a practical ECT system, there are three main sources of stray capacitance which affect the capacitance measurement: screened cable, CMOS switches and sensor screen [12,13]. A 1 m long screened cable connecting the sensing electrode to the measuring circuit introduced about 100 pF of stray capacitance. Typically, the input capacitance of a CMOS switch that is used to select the electrode mode is 8 pF. Besides, the sensor screen outside the sensing electrodes is unable to eliminate all the external noise, and thus contribute to the stray capacitance. The total stray capacitance is about 150 pF, which is much larger than the measured capacitance. Additionally, the stray capacitance may vary with cable movement, ambient temperature changes, component variation and external or internal electric field changes.

In most of the previous research regarding ECT, the signals from the sensor electrodes are usually connected to the signal conditioning circuit by using coaxial cable. Coaxial cable is able to shield disturbance or stray capacitance and thus introduced a very low noise solution. However, the cable connecting the measuring electrode and signal conditioning circuit introduced the most stray capacitance. Therefore, the connecting cables should be as short as possible, and the best solution is not to use cable at all, as implemented in this research. In order to achieve the lowest resistance level for the connection from measurement circuit to electrodes, each of the electrodes is connected to a signal conditioning circuit via 1.0 mm pitch PCB connectors as shown in Figure 8. By comparing with the traditional method which uses coaxial cable, the sensor plate now is just located 10 mm away from the conditioning circuit. Output signal from the sensor plate flows into AC based capacitance measurement circuit is measured in order to get the capacitance value in between the excitation electrode and receiving electrode.

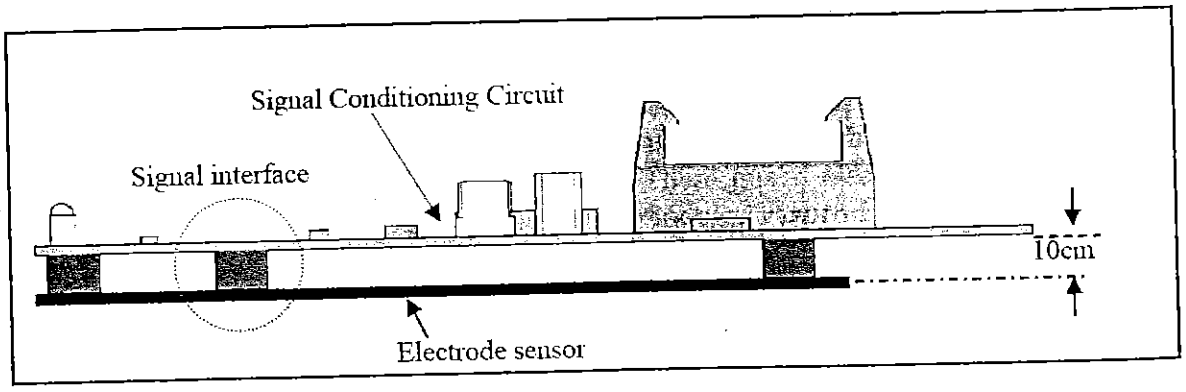

FIGURE 8. Sensing module

Each of the signal conditioning circuits is unique, and is able to work independently because all the measuring operations are controlled by a single microcontroller on the circuit. And each of the circuits consist of signal switching circuit, signal detection and amplifier circuit, absolute value circuit, low pass filter circuit, programmable gain amplifier (PGA), analog to digital converter circuit and a microcontroller control unit. The desire sequence operation of electrode's signal selection, measuring data and conversion data is depended on programming in the microcontroller. The electrodes sensor is designed in a way that it can be plugged directly onto the PCB sockets of the signal conditioning circuit becomes a single sensing module.

These sixteen boards are interconnected by using a 26 way IDC cable. This design had eliminated the need to use cables to connect the electrodes and signal conditioning circuits. Besides, this design is able to cut down the maintenance cost of the system. In the case where only one sensing module is malfunctioning, users can simply change it by plugging out the board and replace it with a new board. Figure 9(a) shows the block diagram of a sensing module and Figure 9(b) shows the actual design. Figure 10 shows the complete ECT signal conditioning system with 16 sensing modules.

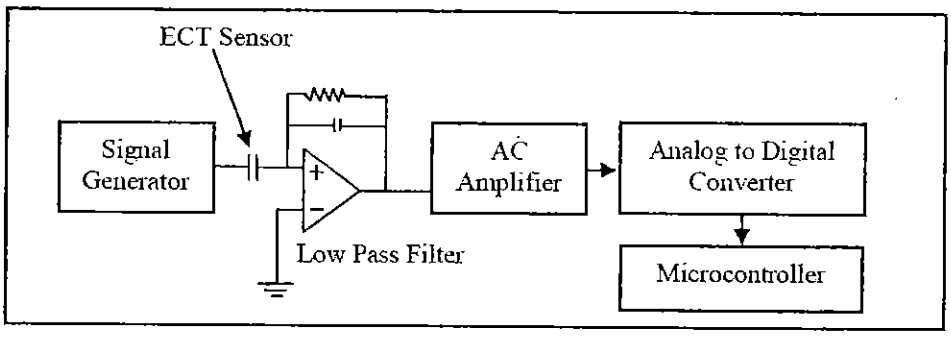

(a)

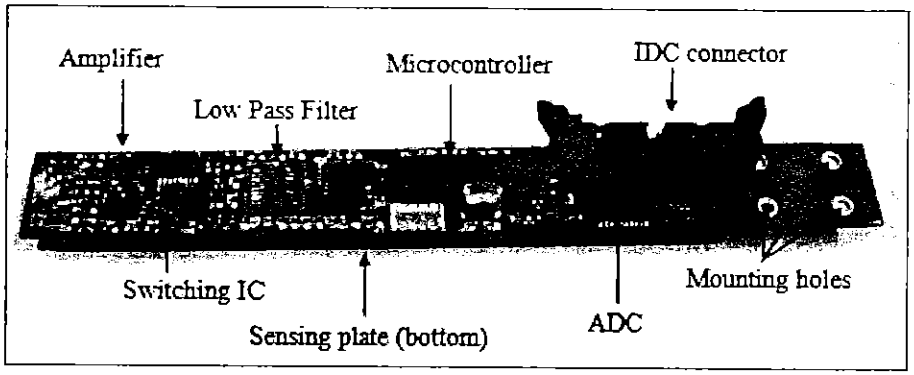

(b)

FIGURE 9. (a) Block diagram of a sensing module and (b) actual sensing module design

The signal conditioning system will measure the capacitance produced by the electrode pairs when a 500 kHz sine wave voltage with the amplitude of 29 $V_{p\text{-}p}$ is injected to one of the electrode pair. With a 500 kHz excitation signal, the circuit has good linearity and stability [14]. The determination of which electrode that will be injected with sine-wave

is controlled by switching and controlling unit. In the receiving electrodes, the signals will be conditioned through several stages, including the AC based capacitance measuring circuit, amplifier circuit, AC to DC converter circuit and filter circuit.

5. **ECT Measurement Circuit.** The measurement electronics is developed following the AC-based capacitance transducer architecture, which has been widely used in recent years due to its immunity to stray capacitances. The diagram of this module is presented in Figure 9(b). The electrodes formed by the segments that compound the sensor are treated, by pairs, as capacitances of unknown value C_x, which must be measured.

5.1. **Switching circuit.** The analog switches required for connecting the electrodes to the different stages of the system are part of a switch array designed for driving the different segments that form the sensor. This makes them to act either as source electrodes, thus being connected to the function generator module, as detector electrodes, being then connected to the measurement electronics, or as free electrodes, leaving them floating in this case. For this work, the CMOS analog ADG453BR chip has been selected.

The signal switching is controlled by a switching circuit that formed by a CMOS analog switches and microcontroller that controls it. The main function of this switching circuit is to control the status of the electrodes so that each electrode can be selected as either the source or detecting electrode. Each set of signal conditioning circuit needs a switching circuit. Thus, the configuration of the switching circuit in this ECT system is as shown in Figure 11.

In the excitation mode, switches $S1$ and $S2$ are closed, while switches $S3$ and $S4$ are open. Hence, the sine wave signal from the function generator can be flown to the electrode and the capacitance measuring circuit is disconnected from the electrode. In the detection mode, switches $S3$ and $S4$ are closed, while switches $S1$ and $S2$ are open. The switch $S3$ connects the coupling capacitance to earth and eliminating its effect on the inter-electrode capacitance measurement. However, due to the fact that switch coupling capacitance exist in CMOS analog switches, the signal from function generator is not totally separated from the electrode. This is where $S3$ takes an important role to flow the signal mentioned above to earth. Signal obtained from the electrode will be measured by the capacitance measuring circuit through $S4$.

5.2. **Detector and amplifier circuit.** In selecting and designing a capacitance measuring circuit, the stray-immune AC capacitance measuring circuit was selected. A stray-immune AC capacitance circuit measures only the capacitance between the selected pair of

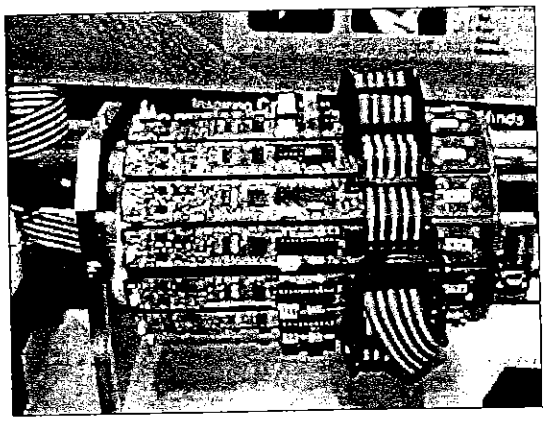

FIGURE 10. Complete ECT sensing module

electrodes, and is insensitive to the stray capacitance between the selected and redundant electrodes and those between the selected electrodes and earth.

Output signal from the sensor plate flows into AC based capacitance measurement circuit is measured in order to get the capacitance value in between the excitation electrode and receiving electrode. An AC-based capacitance measuring circuits using an operational amplifier (Op-Amp) with resistor feedback, which directly measure the AC admittance of an unknown capacitance. In this research, the detector and ac amplifier circuit in used is shown in Figure 12.

From Figure 12, C_x is a standalone capacitance with an unknown dielectric property in between the plate. Since C_{S1} is directly driven by the voltage source, it has no effect on the measurement of C_x provided that the output impedance of the voltage source is small enough. C_{S2} has no effect on the measurement of C_x because the feedback point

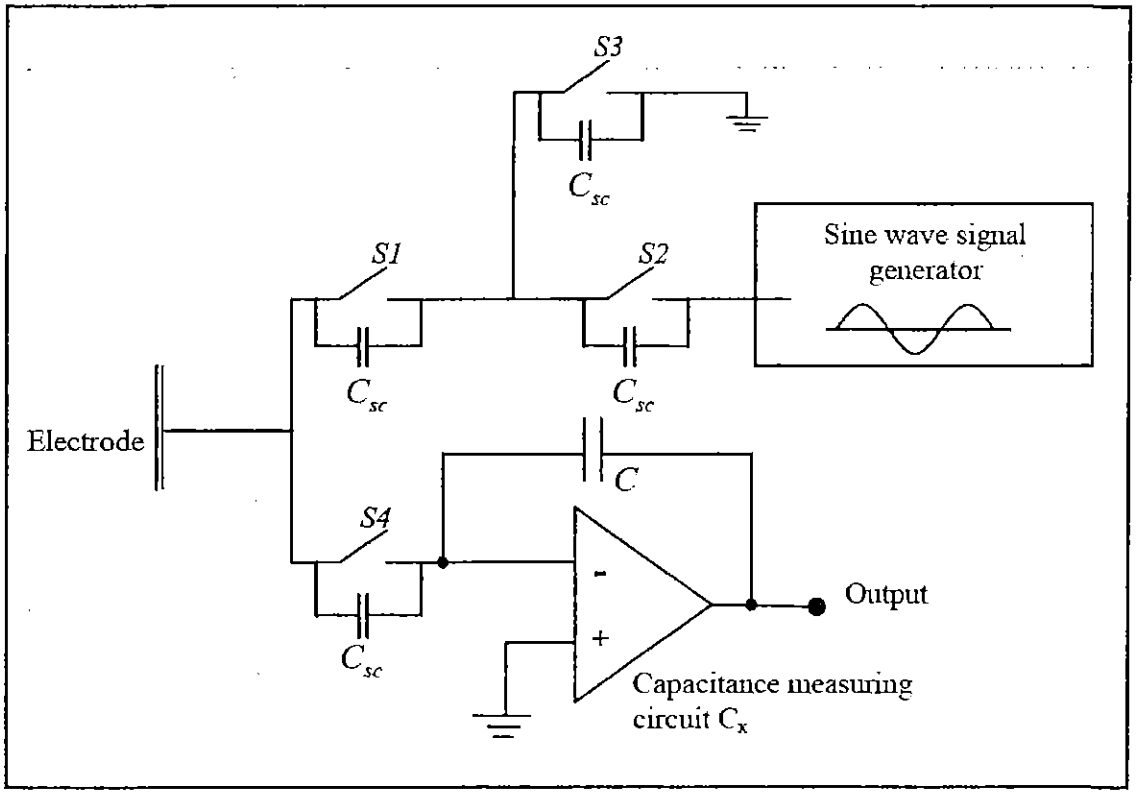

FIGURE 11. The circuit arrangement of four switches for electrode selection

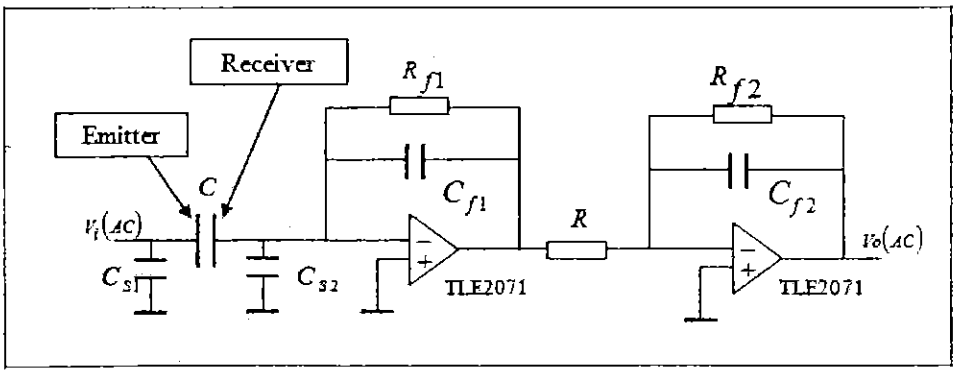

FIGURE 12. Detector circuit and AC amplifier circuit

of the Op-amp is kept at virtual earth and there is no potential difference across C_{S2}. Therefore, this capacitance measuring circuit is inherently stray-immune. The excitation voltage V_i is applied to the unknown capacitance C_x (V_i is the excitation voltage applied to the source electrode, which is obtained from the function generator module). A wide bandwidth operational amplifier, with a feedback capacitance C_f and a feedback resistance R_f, convert the current into an ac voltage, V_0 given by;

$$V_0 = -\frac{j\omega C_x R_f}{j\omega C_f R_f + 1} V_i \tag{1}$$

where ω is the angular frequency of the excitation voltage (sine wave source). When the capacitance feedback is selected to be dominant, i.e., $\frac{1}{\omega C_f} \ll R_f$, as in Equaton (1) becomes;

$$V_0 = -\frac{C_x}{C_f} V_i \tag{2}$$

Equation (2) is an approximation of the real output of the stage formed by the Op-Amp, and it is valid only under the condition $f \gg f_0$, being $f_0 = 1/(2\pi C_f R_f)$ and f the frequency of the excitation signal [15]. In this case, f was settled at 500 kHz. This AC signal is amplified further by an AC amplifier to accommodate a large range of capacitance values.

5.3. **AC to DC converter circuit.** The input signal V_i of the capacitance transducer is the sine wave generated by the function generator. Thus, the output signal V_0 is a sine wave as well, whose amplitude depends on the unknown capacitance C_x. In order to obtain the value of this amplitude, AC to DC converter is used. Despite its simple circuitry, the outputs are considered fast among the available circuit. This is to enable the signal to be directly interfaced with the microcontroller for data-sending to computer. Basically, the AC to DC converter circuit adapted is easily made absolute value circuit.

The output of this absolute value circuit is connected directly to the microcontroller, whose internal ADC will provide a digitized measurement for both the V_i and V_0 amplitudes, from which the final value of the inter-electrode capacitance can be obtained. Therefore, the combination of the classic AC-based capacitance transducer and the absolute value circuit converter results in a stage that provides a DC output signal directly related to the unknown capacitance C_x, and that can be easily digitalized and processed by the microcontroller.

5.3.1. *Absolute value circuit.* Absolute value circuit processes the output voltage to be equal to the input voltage without regard to polarity. As an example, a +6.2 Volts input and a −6.2 Volts input both produce the same (typically +6.2 Volts) output. The schematic diagram in Figure 13 shows the possible way. The first stage of this circuit is a dual half-wave rectifier. For a positive input signal, the output goes in a negative direction and forward-biases D_1. This completes the feedback loop through R_2. Additionally, the forward voltage drop of D_1 is essentially eliminated by the gain of the Op-Amp. That is, the voltage at the junction of R_2 and D_1 will be the same magnitude (but opposite polarity) as the input voltage.

When a negative input voltage is applied to the dual half-wave rectifier circuit, the output of the Op-Amp goes in a positive direction. This forward-biases D_2 thus completes the feedback loop through R_3. Diode D_1 is reverse-biased. In the case of the basic dual half-wave rectifier circuits, the voltage at the junction of R_3 and D_2 is equal in magnitude (but opposite in polarity) to the input voltage. In the case of the circuit in Figure 10, however, this voltage will be somewhat lower because of the loading effect of the current

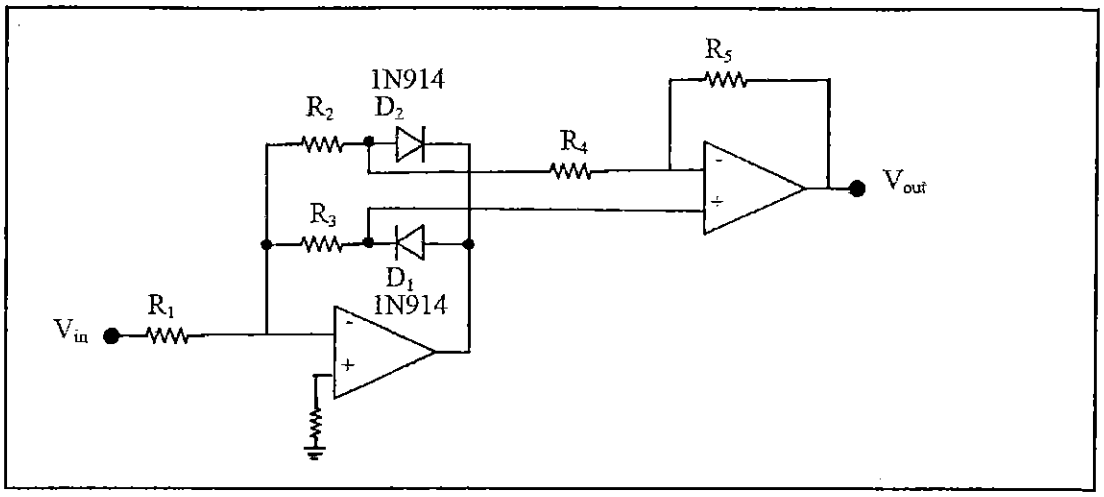

FIGURE 13. Absolute value circuit

flowing through R_2, R_4 and R_5. The outputs from the dual half-wave rectifier circuit are applied to the inputs of a differential amplifier circuit. Since the two half-wave signals are initially 180° out of phase and since only one of them gets inverted by amplifier A2, it can be concluded that the two signals appear at the output of A2 with the same polarity. In other words, both polarities of input signal produce the same polarity of output signal. By definition, this is an absolute value function. Next, the absolute value circuit was combined with first order low pass filter to reduce noise and to get clean DC output from AC input voltage.

5.3.2. *Low pass filter.* A low pass filter circuit must be used to eliminate all the noises. The circuit diagram is shown in Figure 14.

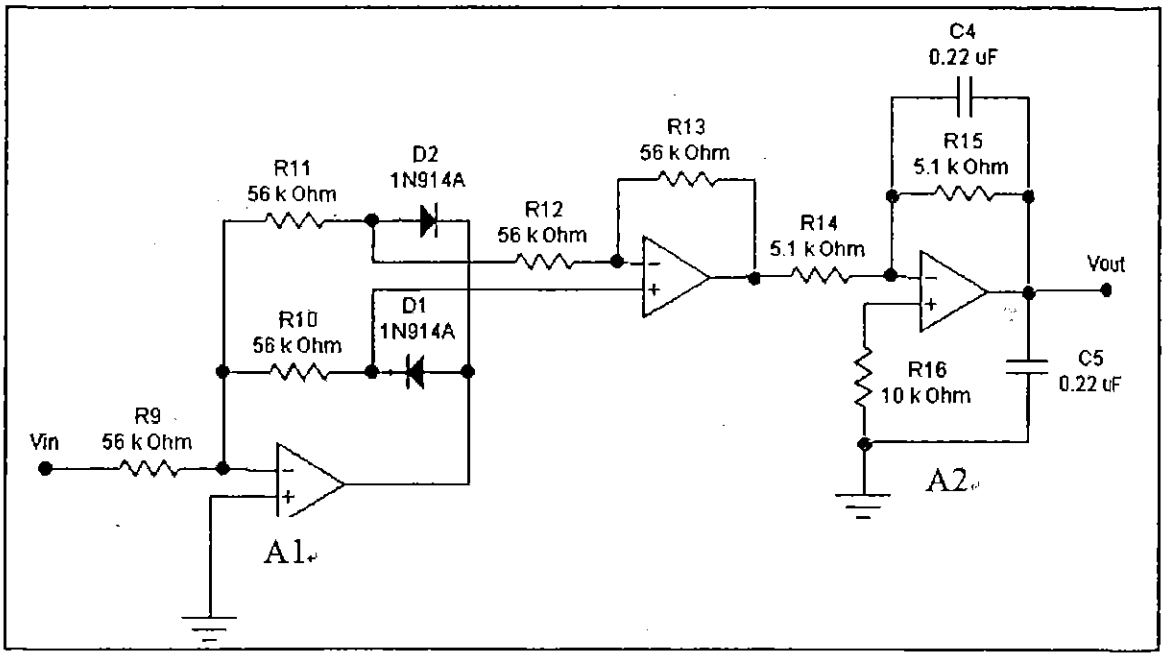

FIGURE 14. Application of low pass filter on the absolute value circuit

As shown in the circuit diagram, all resistor values are the same in the absolute value circuit, thus the calculations for design are fairly straightforward. All the parameters

involved in this circuit are carefully considered and tested for the best performance. Generally, the circuit was designed according to the following specifications:

i. Input voltage approx. $-5.0\ \mathrm{V} \leq V_{\mathrm{in}} \leq 5.0\ \mathrm{V}$.
ii. Input impedance $> 20\ \mathrm{k}\Omega$.
iii. Frequency range 350 kHz to 500 kHz.

Slew rate and small signal bandwidth are investigated as the basis for Op-Amp selection. The required unitygain frequency for A2 can be computed with the equation as follows:

$$\begin{aligned} f_{\text{unitygain}} &= BW \times A_v = BW\left(\frac{R_5}{R_2 + R_4} + 1\right) \\ &= 500\ \text{kHz}\left(\frac{56\ \text{k}\Omega}{56\ \text{k}\Omega + 56\ \text{k}\Omega} + 1\right) \\ &= 750\ \text{kHz} \end{aligned} \tag{3}$$

The selection of resistance must be according to specific requirement. The minimum value for all of the resistors is determined by the required input impedance. The maximum value is limited by the non-ideal characteristics of the circuit, but is generally below 100 kΩ. The 56 kΩ was chosen for the project design.

5.4. **Programmable gain amplifier (PGA).** A PGA is used to amplify the signal received with a controllable gain. It is a necessary to control the signal because the data received is in very large range. When one of the electrodes acts as emitter, all the rest electrodes will act as receiver. A receiver that is located nearest to the emitter will get a very large signal. In order to make sure the signal voltage is in measurable range, it must be amplified with a small gain. For the farthest opposite electrode pair, the receiver will receive a very small signal; hence, a large gain must be applied to the signal.

A high speed programmable gain instrumentation amplifier, PGA206 IC has been applied in the system. The PGA206 has 4 gains selection, which are 1, 2, 4 and 8 V/V. It is digitally programmable and it is ideally suitable for data acquisition system. The gains are selected by two CMOS/TTL compatible lines, which mean it can be easily controlled by a microcontroller. The IC itself is laser-trimmed for low offset voltage and low drift.

5.5. **Analog to digital converter (ADC).** Since all the outputs from the combination of the previous circuits are analog values, thus an ADC circuit must be applied to the final stage of the circuit before the signals are fed into microcontroller. An ADC10461 provided by National Semiconductor has been applied in this project. The ADC10461 is 10-Bit 600 *nano* seconds ADC with Input Multiplexer and Sample/Hold. The chip only needs a 5 V supply, low power dissipation, no missing codes over temperature and no external clock required. In addition, the maximum sampling rate can achieve to 800 kHz.

5.6. **Microcontroller PIC16F876.** As mention earlier, each sensor module is unique, which can work independently. This is because all the operations on the module are controller by a single microcontroller control unit. A high performance CMOS FLASH 8 bit microcontroller, the PIC16F876 that provided by Microchip has been used in this research. The maximum microcontroller's operation speed is 20 MHz and each instruction cycle is 200 ns.

The microcontroller synchronise all the operations on the sensing module. Generally, it has 3 main functions in the system: interfacing with central control unit, switching electrode sensor either act as source or receiver, controlling IC like PGA and ADC. A complete ECT sensor system in this research consists of 16 electrode sensor modules. Thus, there are total 16 microcontrollers are linked together to a main controller, which

is the central control unit. There are several type of communication methods available in microcontroller can be used, but in order to achieve the most highest speed, a special communication method has been create by using five digital channels. In order to identification the sensing module, each of the electrode sensors has its own pre-programmed address. The first digital channel control on source channel selection and the rest four digital channels assign the module's address. So that, an electrode will be selected if the last four channel state is matched its own address. For example, if all the last four channels are low state, the electrode at address 0000 is chosen.

The gain selection for PGA has been pre-programmed in every sensing module. Depend on the receiver electrode location; if the emitter electrode is located far away, the bigger gain is selected to amplify the signal. However, these data will then be normalized in software.

The microcontroller keeps scanning the command changes on the data bus. If the first channel's state is high, and the address bus is matched to an electrode, the microcontroller on the module will receive the command and control the sensing module to become an excitation electrode. At the same time, all the rest electrodes which are not been selected will process the measurement operations. The measurement operations consist of switch the electrode to become a detector electrode, apply gain to the signal before ADC, and do the conversion data on ADC. If the first channel's state is low, and any one of the sensing module match the address represent by the last four channels, then the central control unit now can read the 10 bits ADC data on the selected sensing module.

5.7. **Function generator.** As mentioned earlier, the basic principle of electrical capacitance tomography system is revolved by exciting a sine wave at one of the electrode, and received by all the other electrodes. Therefore, a function generator has been developed in order to reduce the cost of the system. The function generator developed is able to produce sine wave, triangular wave and square wave. However, only sine wave generated will be used in this ECT system. This function generator can produce sine wave up to 29 $V_{p\text{-}p}$. The frequency of the sine wave generated can be varied from around 100 kHz up to about 1 MHz. In the case of electrical capacitance tomography system's usage, sine wave with characteristic as above is sufficient.

In this system, a chip from Maxim, MAX038, is used. The MAX038 is a high frequency and precision function generator which produce triangle, saw tooth, sine, square and pulse waveforms with a minimum of external components. The output frequency can be controlled over a frequency range of 0.1 Hz to 20 MHz by an internal 2.5 V band gap voltage reference and an external resistor and capacitor. The output signal for all waveforms is a 2 $V_{p\text{-}p}$ signal that is symmetrical around ground. The output from the chip is fed into an amplifier circuit to produce a waveform of about 20 $V_{p\text{-}p}$. Figure 15 shows the connection for the function generator chip, MAX038.

A suitable Op-Amp chip is selected to amplify the signal from function generator. Slew rate and small signal bandwidth are investigated as the basis for Op-Amp selection. The required unity gain frequency for the Op-Amp can be computed with the equation as follows:

$$\begin{aligned} f_{\text{unitygain}} &= \text{Bandwidth} * \text{gain} \\ &= 500 \text{ kHz} * 10 \\ &= 5 \text{ MHz} \end{aligned} \tag{4}$$

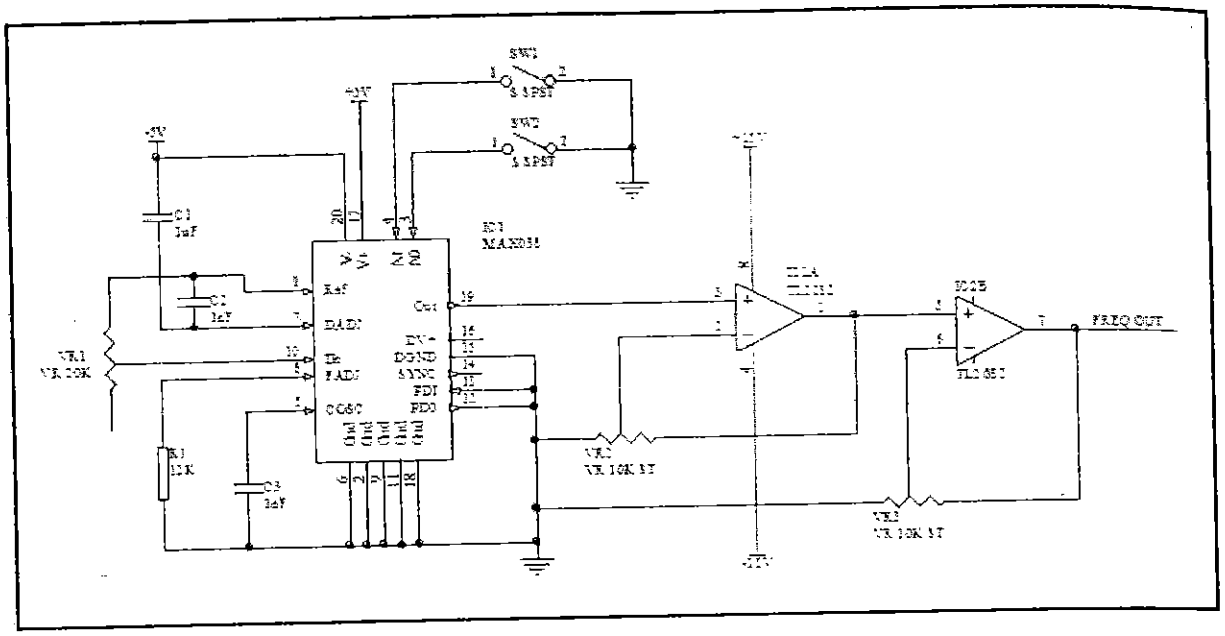

FIGURE 15. Connection of MAX038

The required slew rate for the Op-Amp can be computed as follows:

$$\begin{aligned} \text{Slew rate} &= \pi * f * V_{0(\max)} \\ &= \pi * 500 \text{ kHz} * 20 \text{ V} \\ &= 31.42 \text{ V/us} \end{aligned} \tag{5}$$

TLE 2082 is chosen as the amplifying Op-Amp in this function generator circuit. It has the bandwidth of 10 MHz and slew rate of 45 V/us. which is more than sufficient for the usage of this function generator circuit.

5.7.1. *Function generator output.* The function generator developed in this research is able to produce waveform from below 100 kHz to more than 1 MHz. This function generator can generate 3 types of waveform. which are sine wave. square wave and triangular wave. However, only sine wave is used in this research. Therefore, this section will only discuss the sine wave generated by the function generator developed. Figure 16 shows sine wave that is in used in this research.

The function generator developed in this research is able to generate wave form from 87.93 kHz to 1.437 MHz. In fact, the function generator chip used in this research (MAX 038) is able to produce waveform from around 50 Hz to about 20 MHz. However, the circuitry of the function generator part in this research had restricted the chip to produce such a wide range of waveform frequency. Nevertheless. the frequency needed for this ECT system will not exceed the limitation of the function generator developed. As mentioned by W. Q. Yang et al. in year 1994, the capacitance measurement circuit has good linearity and stability with a 500 kHz excitation signal. This is the reason that 500 kHz sine wave is used as the excitation signal in this research.

6. **Interfacing between Sensor to Computer.** Finally, a user software interface based on Visual Basic has been developed for the instrument. From this interface, the user can perform simple actions, such as selecting the status of the individual segments (source, detector or free-segment), as well as to request a complete set of measurements, from which the image reconstruction will be carried out.

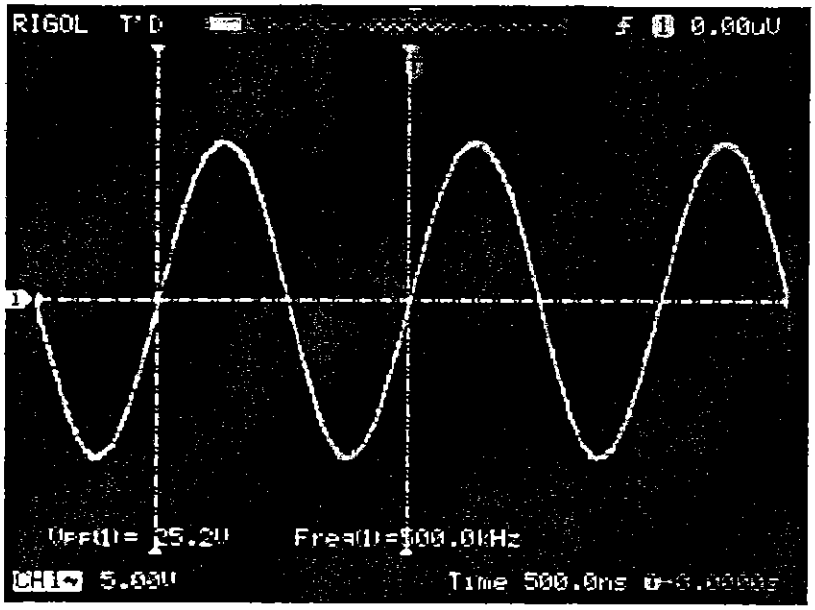

FIGURE 16. Frequency output from function generator

The output data measured from the measurement system needs to be transferred to computer for the process of image reconstruction. There are two factors that must be considered when interfacing the sensors with computer, which are digitization of sensor readings and the gateway of data transferring. Circuits such as multiplexing circuit, analog to digital conversion circuit or buffering circuit may be needed in order to digitize the analog signals obtained in the measurement system to digital data that is suitable for PC interfacing. As for the gateway of data transferring, it can be done by using serial communication such as USB, Ethernet or parallel communication such as printer port. In this case, circuits are required to control the interface.

In order to simplify the system development, industrial standard computer data acquisition system (DAS) is usually implemented in the process tomography system. The general function provided by industrial standard DAS include the multiple channels switching capacity, analog to digital converter (ADC), digital to analog converter (DAC), digital input, digital output, operation of computer interrupt and direct memory access (DMA) and storage of acquired data. One example of the DAS that is frequently used in process tomography system is DAS1802HC from Keithley. This DAS has been used by T. C. Tat [12], A. Rahim et al. [16] and Pang [17]. The use of DAS simplified the procedure of data acquisition as simple as wiring the analog signals to the DAS terminal. It is undeniable that the use of DAS has simplified the design of a system. However, this fact comes with a condition. The cost of developing such a system will increase considerably due to the fact that a DAS is quite expensive. Besides, the system will not be a convenient system for users because users will need to plug the DAS into their PCs, configure the DAS and troubleshoot any problems arise from the DAS in order to use it.

Other than that, ECT system does not need all the functions provided by an industrial standard computer data acquisition system. The most important features that an ECT system needs are the analog to digital conversion and the gateway to transfer the digital data to PC. The speed of the data acquisition system developed must be high enough to support real time imaging for the system. Consequently, high speed analog to digital converters are used in this research for fast analog to digital conversion. In addition, a high data transfer rate PC communication gateway, Universal Serial Bus (USB) technology is

also implemented in this research. Implementation of USB technology ensures that the time used for data transfer from hardware to PC is fast enough that it will not be the speed constrain of the whole system.

7. **Central Control Unit.** A central control unit is used to synchronize all the operation on collecting measurement data and sending the data to a PC for image reconstruction. A high performance and powerful microcontroller PIC18F4550 has been selected in the research, which is developed by Microchip. Thus, it can act as a standalone Data Acquisition System (DAS) that able to work independently.

The PIC18F4550 has a built-in USB controller. The USB technologies supported by this chip are low speed and full speed USB. It means that the transfer rate of the hardware and PC can achieve a maximum of 1.5 Mbps (low speed) or 12 Mbps (full speed). This USB microcontroller uses a 24 MHz crystal, which working in about 167 ns per instruction cycle. The collected data is sent to PC using Communication Device Class (CDC). This is a device level protocol specification defined by the USB association body. It defines the rules of how a USB host and a USB peripheral should communicate as a communication device. Specifically, the CDC specification defines a wrapper protocol layer around other communication protocols allowing them to be transported over the USB interface. A standardized specification also allows a USB host and a USB peripheral to be developed independently.

In order to make the easiest way for this system to interface to a PC, implementation of RS-232 emulation over USB technique has been used. One of the most advantage by using this technique because the Windows 2000 and XP already come with a driver which provides the RS-232 emulation capability as defined in the CDC specification. The data received in PC will be received by the device driver, and then is retrieved through the software developed for further manipulation. Figure 17 shows the picture of the central control unit.

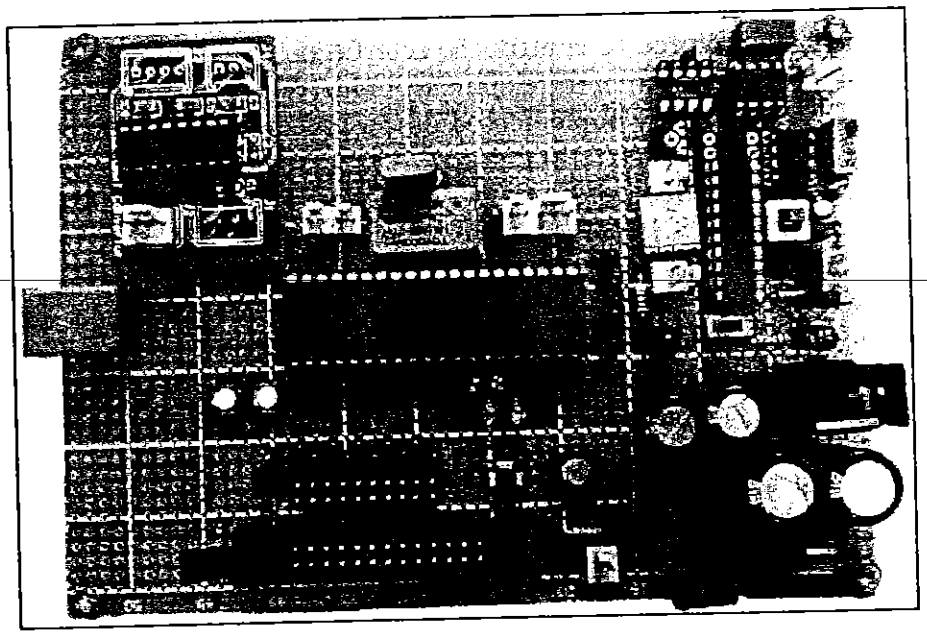

FIGURE 17. Picture of the data acquisition system

There are total of 120 data collected in each measurement cycle. And the data sending to PC in bulk will be much faster than sending in byte. Thus, all the data will be stored in memory before send to PC for image reconstruction. The data received in PC will be

received by the device driver, and then is retrieved through the software developed for further manipulation.

Overall, the hardware is working standalone, which mean that the central control unit will take role to control the whole process after receive instruction from a host PC. The central control unit will keep controlling the measuring operation, collecting data from electrode modules and sending data to host computer for image reconstruction.

8. **Experimental Results.** In this section, a detailed study of system specifications is carried out, with special emphasis in the image quality of the system including sensor design, measurement, reconstruction and imaging of permittivity distributions. The main goal of this section is to demonstrate that the portable ECT instrument presented in this work is able to provide images of high quality for real-time applications. Figure 18 shows the output voltage change if different permittivity is filled inside pipeline. The nearest electrodes output always have the highest sensitivity, thus the distinction of capacitance value is easily affected by flowing material inside pipeline. The comparison obviously shows that the voltage change in between opposite electrode is the lowest.

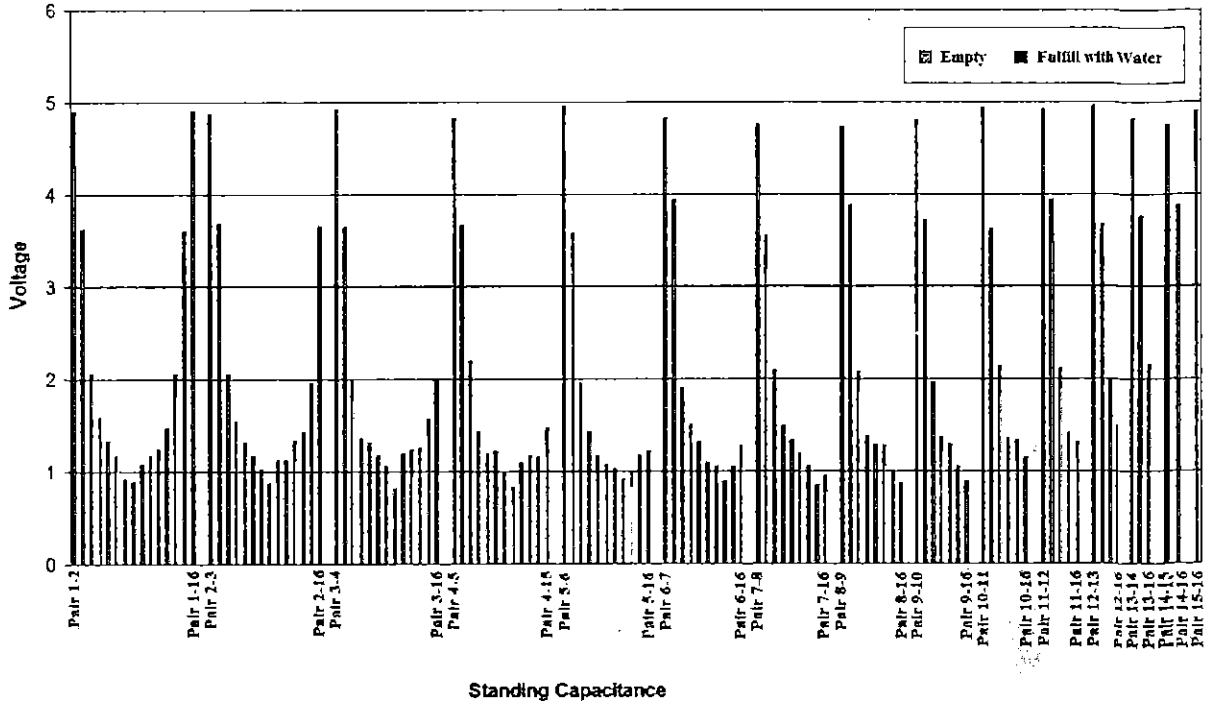

FIGURE 18. Data comparison between low-permittivity and high-permittivity in pipeline

Experiment has been setup to measure the concentration of palm oil and air two phase flows from 10 percent to 100 percent in the step size of 10 percent, shown in Figure 19. In this experiment, palm oil is calibrated as maximum limit in data measurement.

Figure 20 shows the comparison between actual concentration and concentration obtained, the concentration measured is higher than actual concentration at 30% to 80% water. This is due to the range of permittivity change has been decreased and the image reconstruction of two phase flow of palm oil/water shows in Figure 21.

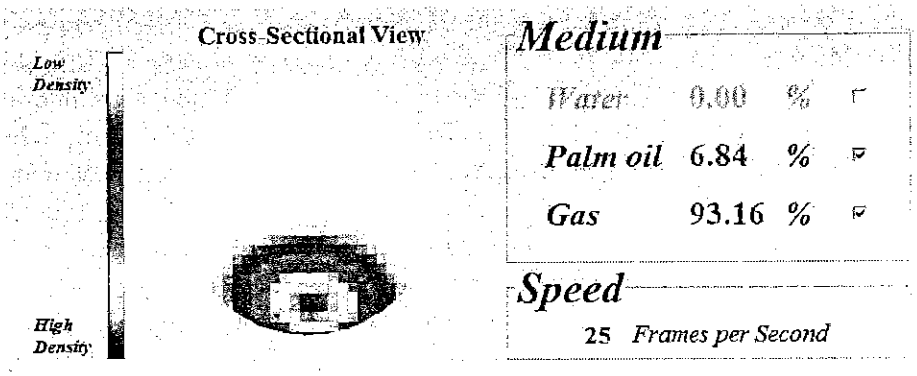

(a) 10% palm oil, 90% air flow

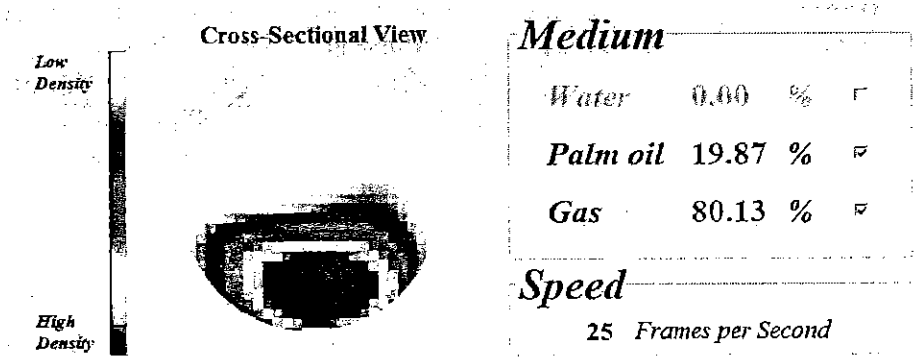

(b) 20% palm oil, 80% air flow

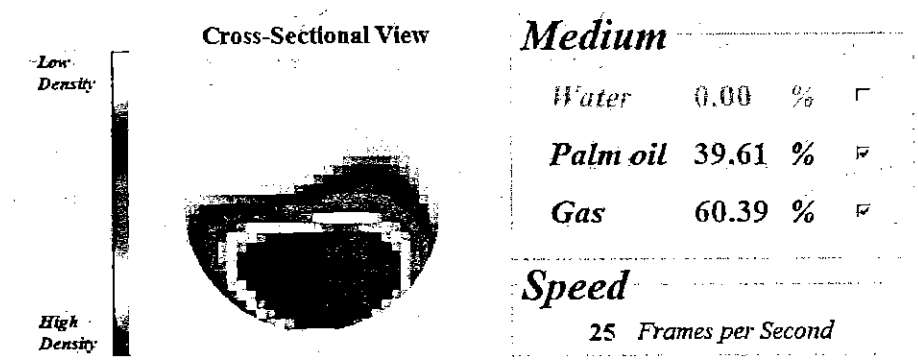

(c) 30% palm oil, 70% air flow

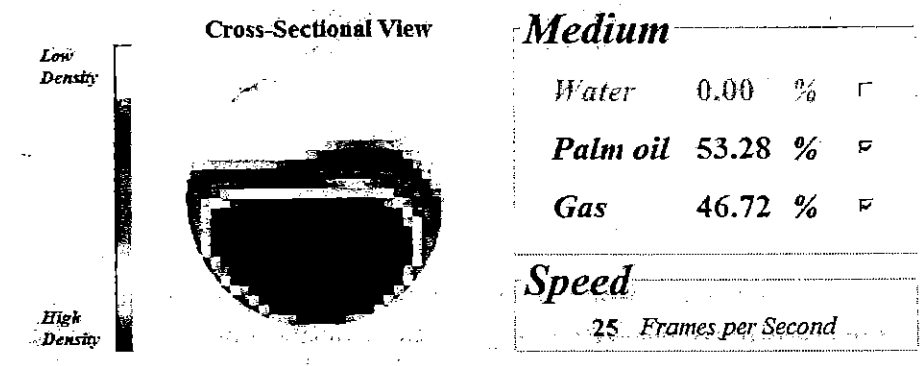

(d) 40% palm oil, 60% air flow

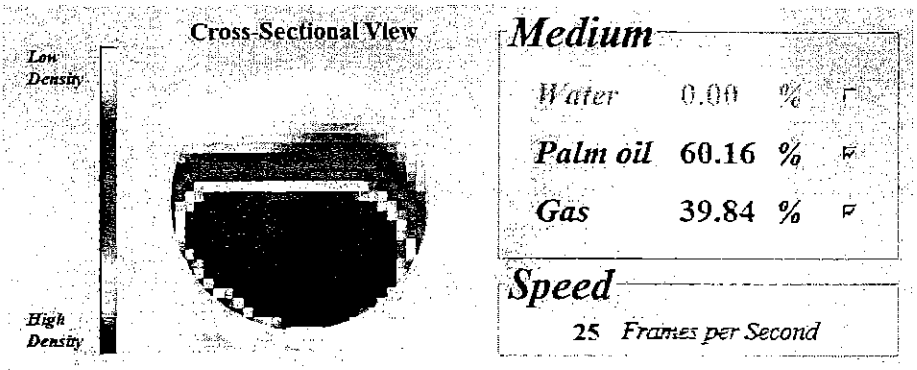

(e) 50% palm oil, 50% air flow

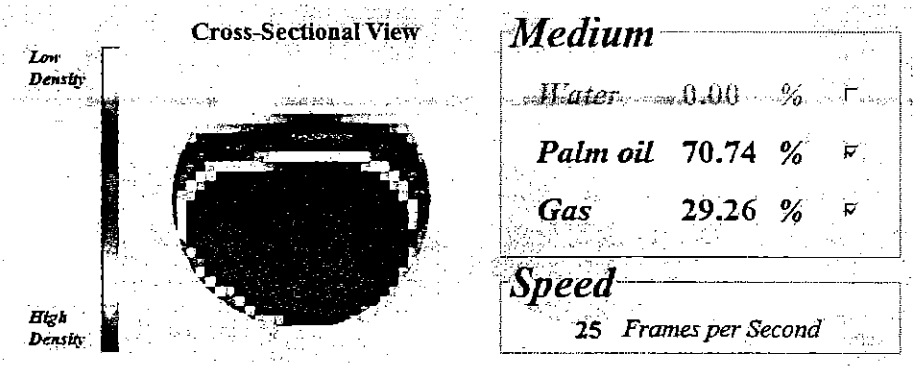

(f) 60% palm oil, 40% air flow

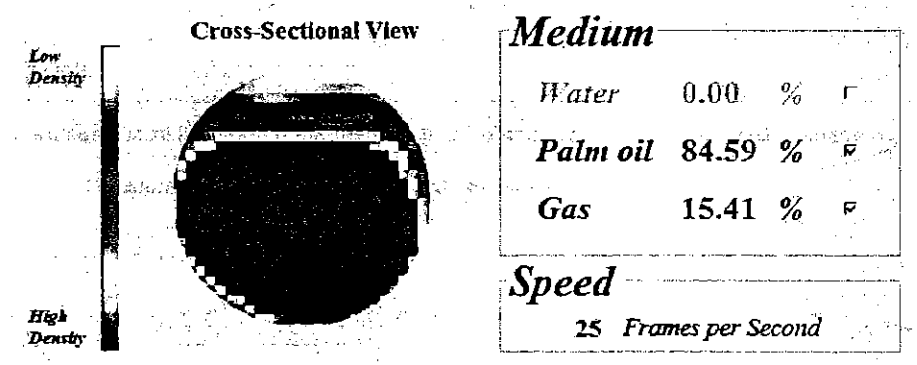

(g) 70% palm oil, 30% air flow

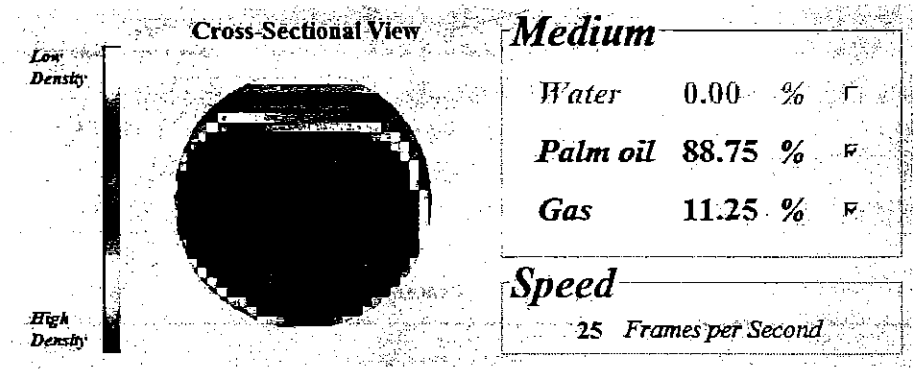

(h) 80% palm oil, 20% air flow

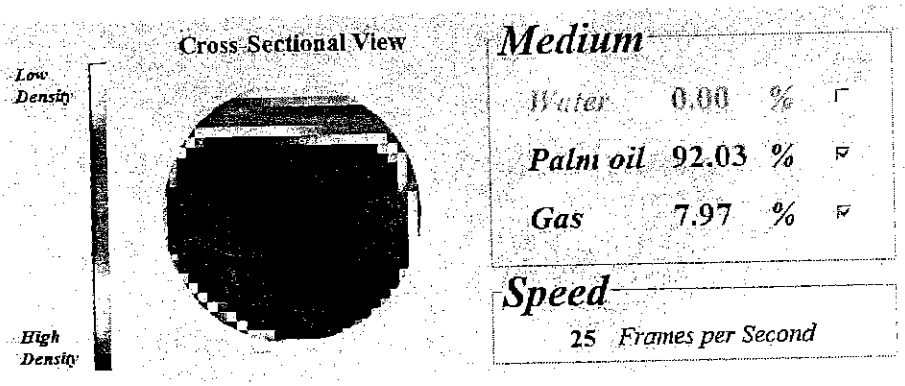

(i) 90% palm oil, 10% air flow

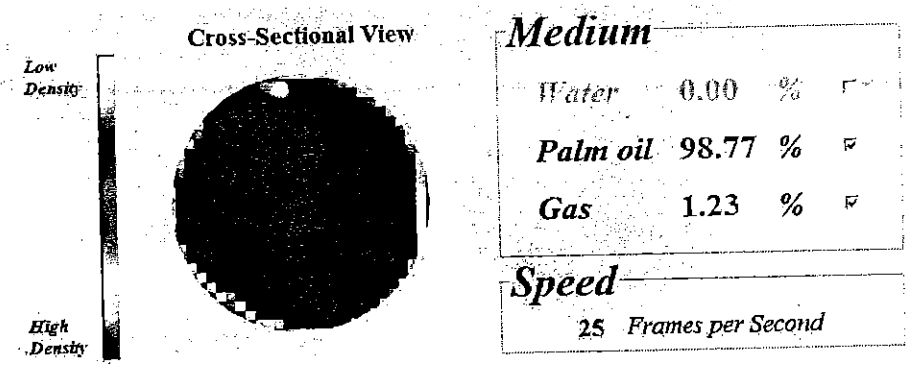

(j) 100% palm oil, 0% air flow

FIGURE 19. Reconstructed image for different flow concentration of palm oil and air two phase flows

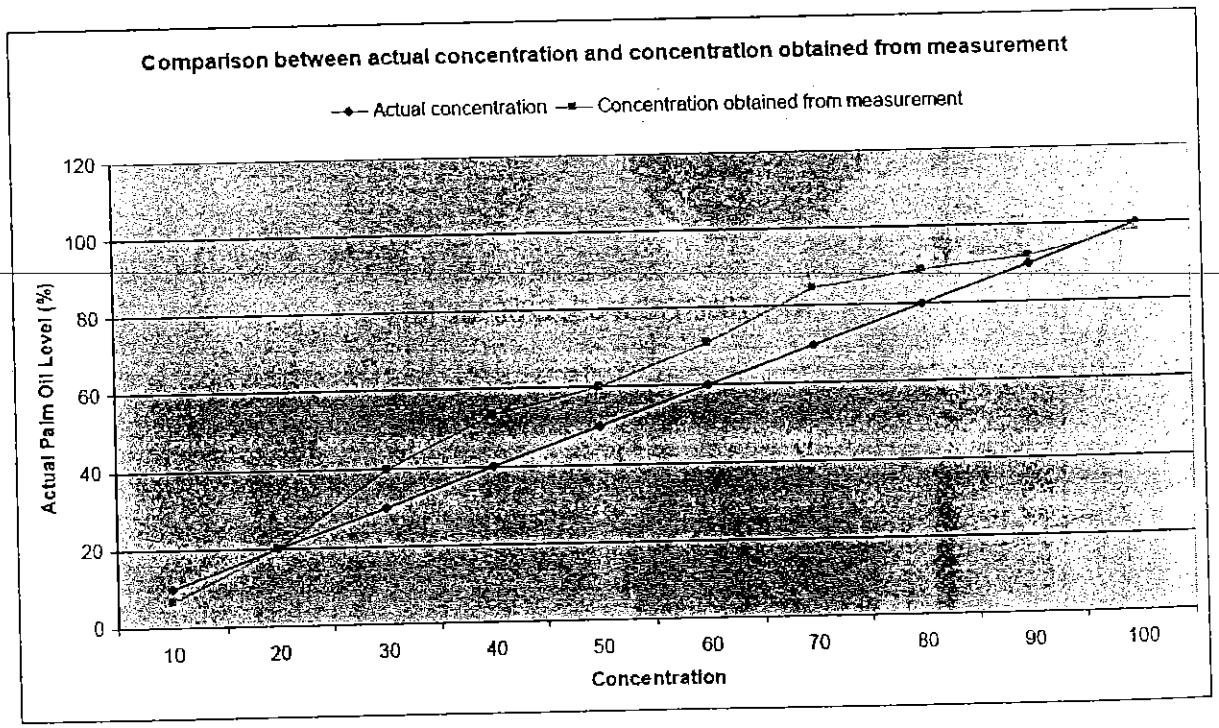

FIGURE 20. Comparison between actual concentration and concentration obtained from measurement for palm oil/air flow

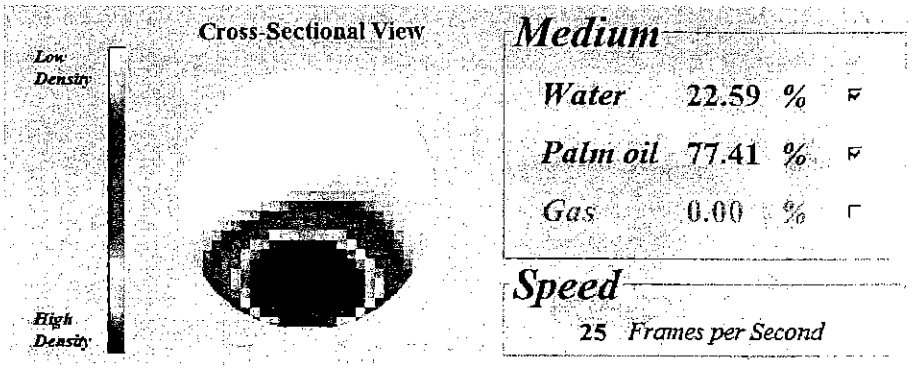

(a) 10% water, 90% palm oil

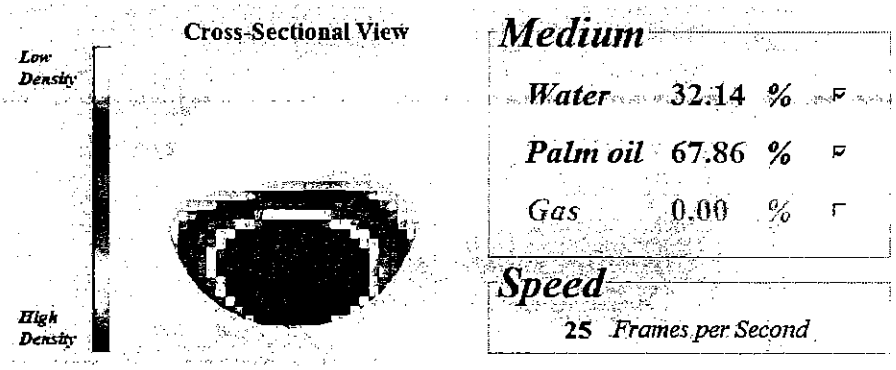

(b) 20% water, 80% palm oil

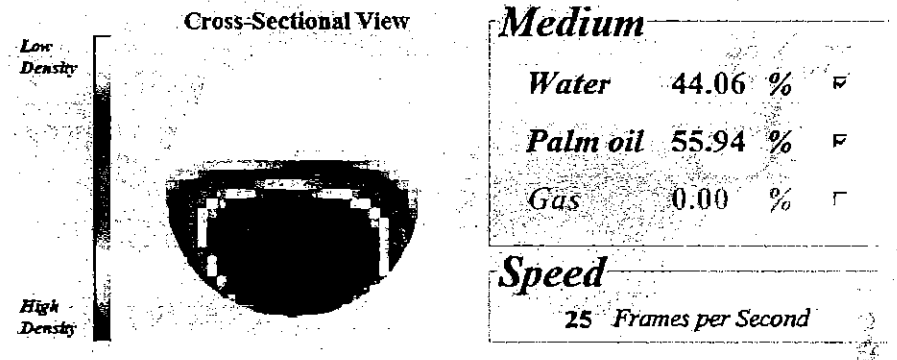

(c) 30% water, 70% palm oil

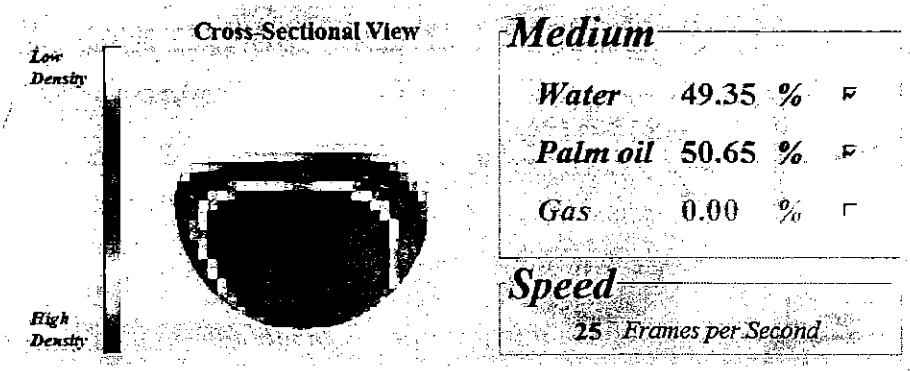

(d) 40% water, 60% palm oil

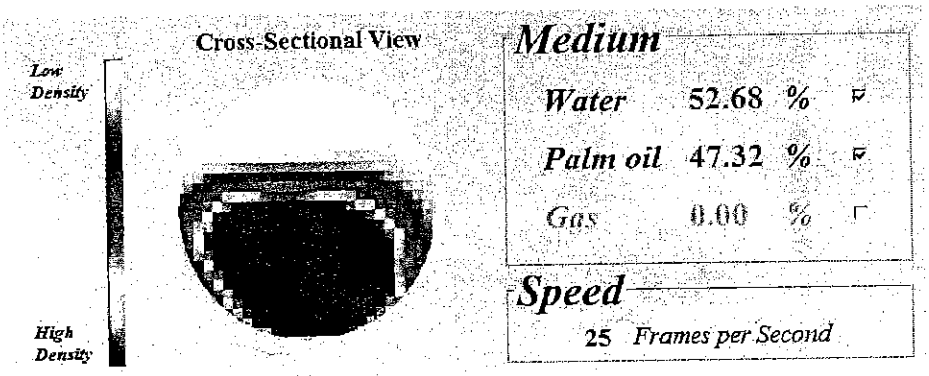

(e) 50% water, 50% palm oil

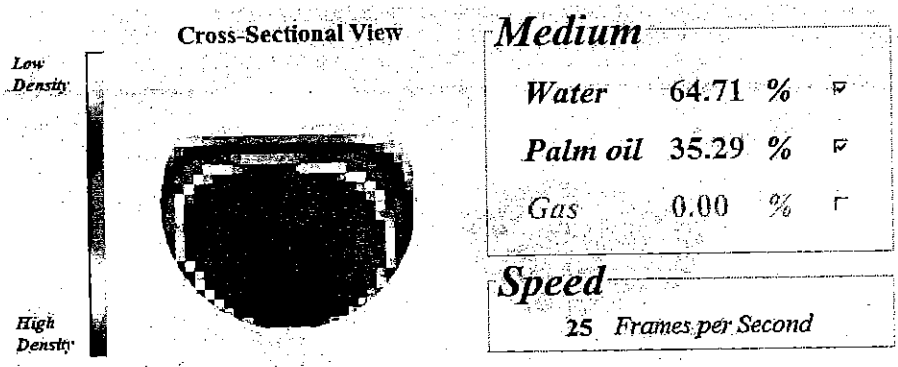

(f) 60% water, 40% palm oil

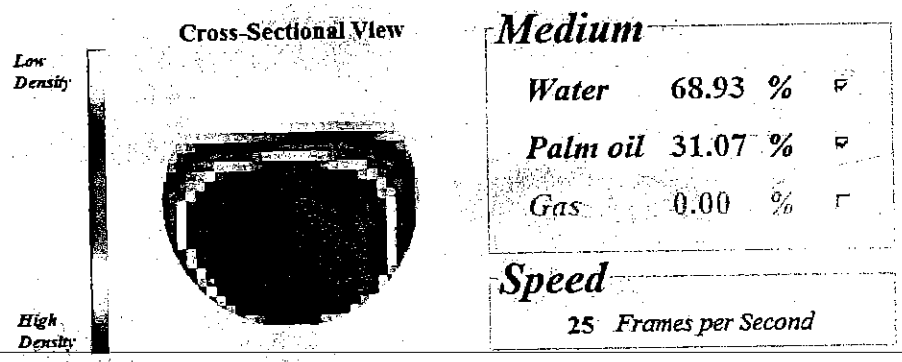

(g) 70% water, 30% palm oil

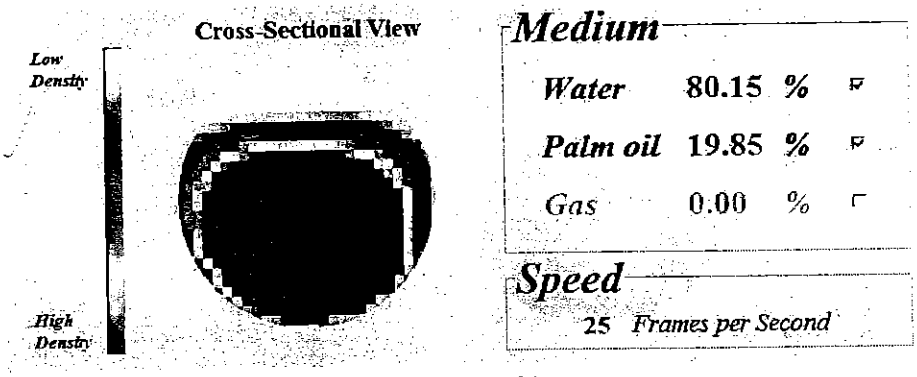

(h) 80% water, 20% palm oil

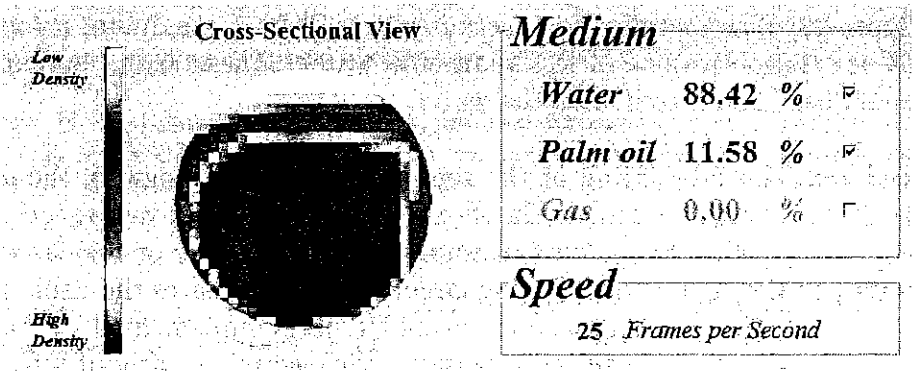

(i) 90% water, 10% palm oil

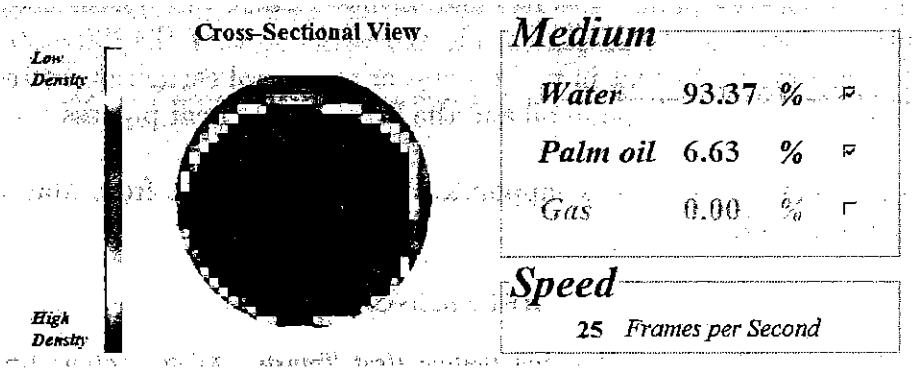

(j) 100% water, 0% palm oil

FIGURE 21. Reconstructed image obtained for different flow concentration of palm oil and air two phase flow (a)-(j)

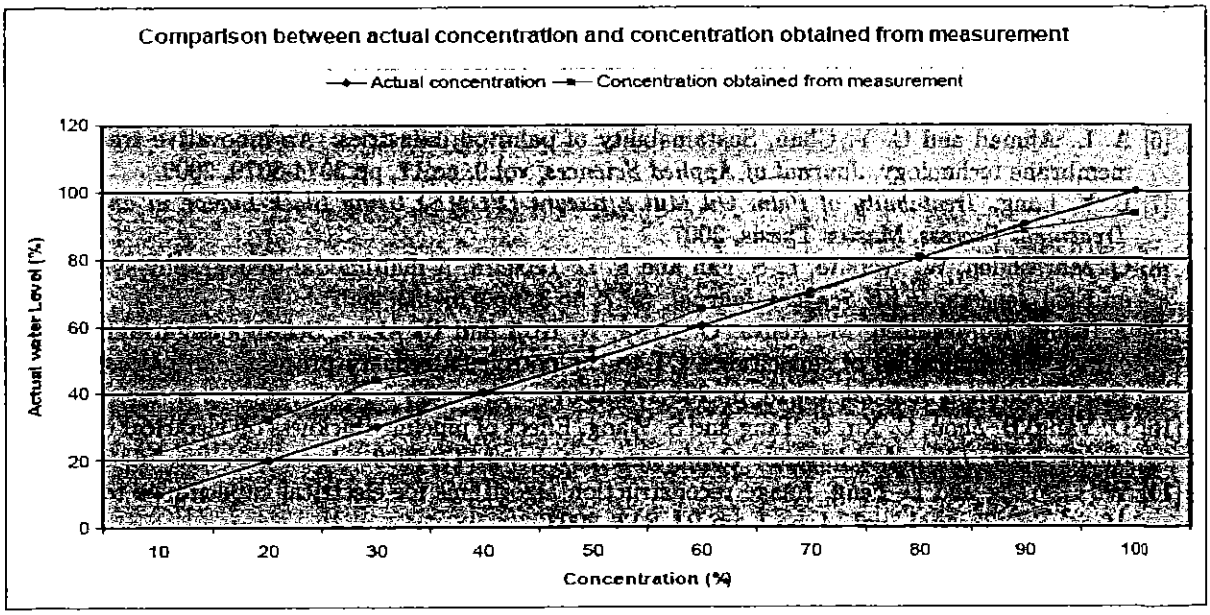

FIGURE 22. Comparison between actual concentration and concentration obtained from measurement for water/palm oil flow

The comparison between actual concentration and the concentration obtained from measurement for water/palm oil flow is shown in Figure 22.

From Figure 22, the concentration measurements show a maximum error of approximately 12% for concentrations of less than 50% water. These errors may arise because some of the oil has been mixed with the water.

9. **Conclusions.** The fabricating of the sensors electrodes, designing the signal conditioning circuit had been described. In short, a portable non-invasive sensor system is designed and fabricated. The system is designed so that it does not use cables to connect the electrodes and the signal conditioning circuit. This eliminates the cable noise. Other than that, stray immune capacitance measuring circuit is implemented so that the circuit measures only the standing capacitance between the electrodes without affected by stray capacitance in the circuit. Linear Back Projection algorithm is applied in producing a good quality tomogram. The system that has been developed is capable to determine the distribution between palm oil, water and air flow. Thus, the system able to visualize the percentage of load waste present inside the vessel so that the data can be used to design better process equipment in mill process or to control certain processes in order to maximize the quality of crude palm oil and the POME treatment process can be improve.

Acknowledgment. This work is supported by Research Grant from Malaysia Government, EScience vot 79025.

REFERENCES

[1] Z. Lin, *Gas-liquid Two-phase Flow and Boiling Heat Transfer*, Xi'an Jiaotong University Press, Xi'an, China, 2003.

[2] R. A. Rahim, Z. C. Tee, M. H. F. Rahiman and J. Pusppanathan, A low cost and high speed electrical capacitance tomography system design, *Sensor and Transducer Journal*, vol.114, no.3, pp.83-101, 2010.

[3] P. Williams and T. York, Evaluation of integrated electrodes for electrical capacitance tomography, *The 1st World Congress on Industrial Process Tomography*, Buxton, Greater Manchester, 1999.

[4] S. Liu, L. Fu and W. Yang, Optimization of an iterative image reconstruction algorithm for electrical capacitance tomography, *Meas. Sci. Technol.*, vol.10, no.7, 1999.

[5] M. Ahmed, *The Use of Microfillter Recovered Palm Oil Mill Enffluent (POME) Sludge as Fish Feed Ingredient*, Master Thesis, 2009.

[6] A. L. Ahmad and C. Y. Chan, Sustainability of palm oil industries: An innovative treatment via membrane technology, *Journal of Applied Sciences*, vol.9, no.17, pp.3074-3079, 2009.

[7] L. Y. Lang, *Treatability of Palm Oil Mill Effluent (POME) Using Black Liquor in an Anaerobic Treatment Process*, Master Thesis, 2007.

[8] Q. Marashdeh, W. Warsito, L.-S. Fan and F. L. Teixeira, A multimodal tomography system based on ECT sensors, *IEEE Sensors Journal*, vol.7, no.3, pp.426-433, 2007.

[9] Z. Tong, T. Masahiro, M. Kenta, O. Ryoji, N. Koji and U. Akira, Sensor design and image accuracy for application of capacitance CT to the petroleum refinery process, *Flow Measurement & Instrumentation Journal*, vol.18, pp.268-276, 2007.

[10] D. Yang, B. Zhou, C. Xu, G. Tang and S. Wang, Effect of pipeline thickness on electrical capacitance tomography, *Journal of Physics: Conference Series*, vol.147, 2009.

[11] W. Q. Yang and L. Peng, Image reconstruction algorithms for electrical capacitance tomography, *Meas. Sci. Technol.*, vol.14, no.1, pp.R1-R13, 2003.

[12] T. C. Tat, *Water/Oil Flowing Imaging of Electrical Capacitance Tomography System*, Bachelor Thesis, Universiti Teknologi Malaysia, 2003.

[13] A. M. Olmos, M. A. Carvajal, D. P. Morales, A. García and A. J. Palma, Development of an electrical capacitance tomography system using four rotating electrodes, *Sensors and Actuators A: Physical*, vol.148, pp.366-375, 2008.

[14] W. Q. Yang, A. L. Stott and M. S. Beck, High frequency and high resolution capacitance measuring circuit for process tomography, *IEE Proc. of Circuit Devices Syst.*, vol.141, no.3, 1994.

[15] J. C. Gamio, W. Q. Yang and A. L. Stott, Analysis of non-ideal characteristics of an AC-based capacitance transducer for tomography, *Meas. Sci. Technol.*, vol.12, pp.1076-1082, 2001.

[16] R. A. Rahim, L. C. Leong, K. S. Chan and J. F. Pang, Hardware implementation of multiple fan beam projection technique in optical fibre process tomography, *Sensor Journal*, vol.8, pp.3406-3428, 2008.

[17] J. F. Pang, R. A. Rahim and K. S. Chan, Infrared tomography sensor configuration using four parallel beam projections, *Proc. of the 3rd International Symposium on Process Tomography*, Lodz, Poland, 2004.

[18] C. Zhou, X. Wei, Q. Zhang and B. Xiao, Image reconstruction for face recognition based on fast ICA, *International Journal of Innovative Computing, Information and Control*, vol.4, no.7, pp.1723-1732, 2008.

[19] J. Pan, C. Zhang and Q. Guo, Image enhancement based on the shearlet transform, *ICIC Express Letters*, vol.3, no.3(B), pp.621-626, 2009.

[20] Y. Zhang, C. Zhang, J. Chi and R. Zhang, An algorithm for enlarged image enhancement, *ICIC Express Letters*, vol.3, no.3(B), pp.669-674, 2009.

[21] W. F. Al Maki, T. Hori, T. Kitagawa and S. Sugimoto, Scene reconstruction from a single image for circular motion blur, *International Journal of Innovative Computing, Information and Control*, vol.6, no.1, pp.103-116, 2010.